Proc. Natl. Acad. Sci. USA
Vol. 89, pp. 6934–6937, August 1992
Biophysics

New transients in the electron-transfer dynamics of photolyzed mixed-valence CO-cytochrome *c* oxidase

(transient absorption spectroscopy/flash photolysis)

ÓLÖF EINARSDÓTTIR*, TIMOTHY D. DAWES, AND KATY E. GEORGIADIS

Department of Chemistry, University of California, Santa Cruz, CA 95064

Communicated by Harry B. Gray, April 21, 1992

ABSTRACT **Electron transfer following photolysis of CO from mixed-valence (cytochrome a^{3+} Cu_A^{2+} cytochrome a_3^{2+}-CO Cu_B^{+}) cytochrome oxidase (ferrocytochrome-*c*; oxygen oxidoreductase, EC 1.9.3.1) was studied on time scales of nanoseconds to milliseconds by multichannel time-resolved optical absorption spectroscopy. In this method, the optical absorption was measured at many wavelengths simultaneously by using an optical spectrometric multichannel analyzer system. The high-quality time-resolved difference spectra showed a large increase on a microsecond time scale in the visible region centered at ≈520 nm and in the UV region centered at ≈390 nm. These absorbance changes were not observed after photodissociation of CO from the fully reduced enzyme and therefore are attributed to intramolecular electron transfer. Simultaneously, there was a blue shift and a small increase in the α band, which is attributed to the reduction of cytochrome *a*. Approximately one-third of the absorbance change at 520 nm can be attributed to reduction of cytochrome *a*. The absorbance changes associated with the 520- and the 390-nm bands are on the same time scale ($t_{1/2} \approx 2$ μs) as the dissociation of CO from Cu_B^{+} reported previously by time-resolved infrared spectroscopy. The position and shape of these bands are reasonable for charge-transfer transitions involving copper(II). We suggest that the absorbance increase at 520 nm, which cannot be attributed to a reduction of cytochrome *a*, may represent a charge transfer involving Cu_B^{2+} accompanying the oxidation of Cu_B^{+} to Cu_B^{2+}. The absorbance increase at 390 nm is also partially attributed to this transition. These results suggest that Cu_B^{2+} may be observed spectrophotometrically in the electron-transfer dynamics of cytochrome oxidase.**

Cytochrome oxidase (ferrocytochrome-*c*:oxygen oxidoreductase, EC 1.9.3.1), the terminal oxidase of cellular respiration, catalyzes the four-electron transfer from cytochrome *c* to molecular oxygen. The enzyme contains two heme A chromophores (cytochromes *a* and a_3) and two redox-active coppers (Cu_A and Cu_B). The energy that is derived from the reduction of dioxygen to water is coupled to active translocation of protons across the membrane and used by the cell to synthesize ATP, the ubiquitous biological energy source (1). Of the four redox active centers, cytochrome *a* and Cu_A are believed to be the primary acceptors of electrons from cytochrome *c*, followed by electron transfer to the site of O_2 reduction, which comprises cytochrome a_3 and Cu_B. However, the details of the mechanism of the dioxygen reduction, how the enzyme functions as a proton pump, and how the proton pumping is linked to electron transfer remain unclear. Adequate understanding of the precise electron-transfer sequence among the four redox-active metal centers would clearly help to elucidate the role of the individual redox centers as electron carriers and perhaps to increase our understanding of how electron transfer may be coupled to proton translocation.

Electron transfer in cytochrome oxidase can be studied by photolyzing CO from the mixed-valence (cytochrome a^3 Cu_A^{2+} cytochrome a_3^{2+}-CO Cu_B^{+}) complex (2–6). This causes a back flow of electrons from cytochrome a_3/Cu_B to cytochrome *a* and/or Cu_A, which has been attributed to a change in the redox potential of the binuclear site when CO binds to or photodissociates from cytochrome a_3 (2). Earlier studies on the electron-transfer reactions of cytochrome oxidase after flash photolysis of the mixed-valence CO–cytochrome oxidase complex have given varying results, and the interpretations regarding which metal centers are involved differ (2–5). Also, absorbance changes were observed that were too fast for the experimental dead time (microsecond time scale) (2–5). Oliveberg and Malmström (6) have reported fast absorbance changes (rate constant of 2×10^5 s^{-1}) both at 445 and 605 nm after photolysis of CO from the two and three electron-reduced complexes. Clearly, measurements on the intermediate oxidation states of the enzyme on a fast time scale can provide new information regarding the rate of electron transfer. In these previous studies (2–6), the changes in absorbance were followed in a kinetic mode at selected wavelengths as a function of time after CO photolysis with a monochromator/photomultiplier system. However, in this mode, if one wants to detect an entire time-resolved UV–visible spectrum rather than a change in absorbance at a single wavelength, the transients at individual wavelengths need to be collected point by point. This method is rather tedious and potentially imprecise, and important information in the time-resolved spectra can be lost depending on the wavelengths selected.

In this paper, we report room temperature multichannel time-resolved UV–visible spectroscopic studies of intramolecular electron transfer in cytochrome oxidase after photolysis of CO from the mixed-valence enzyme. The high-quality transient UV-visible difference spectra on time scales of nanoseconds and microseconds show the unique capability of the optical spectrometric multichannel analyzer system to follow transient intermediates in the electron-transfer and ligand-binding dynamics of cytochrome oxidase. These studies reveal new microsecond time scale ($t_{1/2} \approx 2$ μs) absorbance changes centered at ≈520 nm and ≈390 nm that have not been observed previously in cytochrome oxidase electron-transfer dynamics. We tentatively attribute these changes to a charge-transfer transition involving Cu_B^{2+} and to reduction of cytochrome *a*.

MATERIALS AND METHODS

Cytochrome oxidase was isolated from beef heart by the method of Yoshikawa *et al.* (7). The final product was in 0.1 M sodium phosphate buffer (pH 7.4). The enzyme concen-

The publication costs of this article were defrayed in part by page charge payment. This article must therefore be hereby marked "*advertisement*" in accordance with 18 U.S.C. §1734 solely to indicate this fact.

*To whom reprint requests should be addressed.

tration was determined by using the extinction coefficient of the fully oxidized oxidase at 598 nm, 8.5 $mM^{-1} \cdot cm^{-1}$ in terms of total heme. The mixed-valence CO-bound complex was prepared by incubation of oxidized enzyme under 1 atmosphere (1 atm = 101.3 kPa) CO in the absence of dioxygen for several hours. The fully reduced CO complex was prepared by addition of a small excess of dithionite to a deoxygenated enzyme solution under nitrogen, followed by blowing CO over the solution for 30 min.

The photolysis was accomplished with a DCR-11 Nd:YAG (yttrium/aluminum garnet) laser (532 nm, 80 mJ per pulse, 7-ns duration pulse) with a repetition rate of 2 Hz. The probe beam, a high-power Xenon flash lamp (8), was passed through the sample and filters and then was focused into a spectrograph. For the spectra obtained in the visible region, a 1-mm cuvette was used, with the photolysis beam and the probe beam focused collinearly. For the Soret region, a 10 × 4 mm cuvette was used, and the photolysis was carried out along the 10-mm pathlength, with the sample probed at 90° to the photolysis beam along the 4-mm pathlength. The time-resolved optical absorption signals were detected by an intensified silicon diode array [Princeton Instruments (PI) (Trenton, NJ) IRY-700G]. The optical spectrometric analyzer (OSMA) direct memory access controller (PI, ST-120) digitizes the channels of the OSMA by using a 14-bit analog-to-digital converter. The nanosecond time resolution in these experiments was determined by a pulser (PI, FG-100) that provided a continuously adjustable gate width from 5 ns to 2.5 μs. The spectra obtained at different times after photolysis of CO from cytochrome a_3 were measured by varying the time of the intensifier gate pulse relative to the laser excitation (pump) pulse by using a delay generator. An oscilloscope was used to observe the timing between the pulses. The collected spectra were averaged and transferred to a computer for data analysis. The reported transient difference spectra are an average of 256 single spectra.

RESULTS AND DISCUSSION

Figs. 1 and 2 show the time-resolved difference spectra on nanosecond and microsecond time scales in the Soret and the visible regions, respectively, after photodissociation of CO

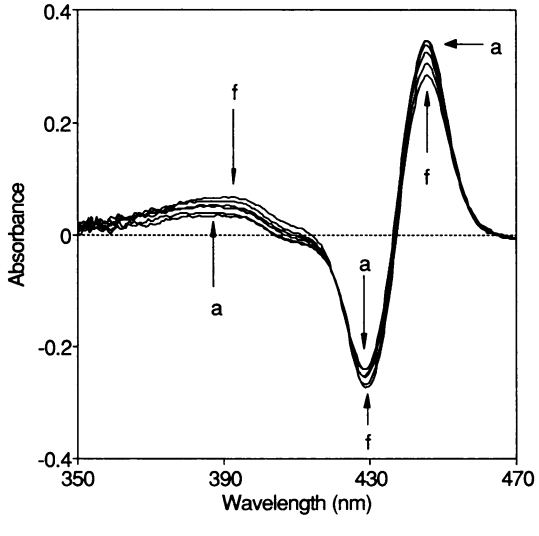

FIG. 1. UV transient difference spectra after photolysis of CO from cytochrome a_3 of the mixed-valence complex. The sample was 23 μM in total heme in 0.1 M sodium phosphate buffer (pH 7.4). A 4-mm pathlength was used. Each spectrum is an average of 256 single spectra. Spectra (in order from a to f) were measured 10 ns (a), 0.1 μs (b), 0.7 μs (c), 1.5 μs (d), 5.0 μs (e), and 50 μs (f) after photodissociation of CO from cytochrome a_3.

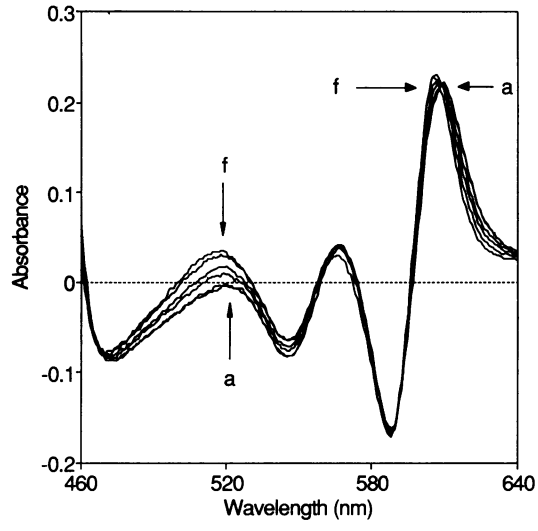

FIG. 2. Visible transient difference spectra after photolysis of CO from cytochrome a_3 of the mixed-valence complex. Cytochrome oxidase concentration was 1.1 mM in total heme, and a 1-mm pathlength was used. Each spectrum is an average of 256 single spectra. Spectra (in order from a to f) were measured 10 ns (a), 0.1 μs (b), 0.7 μs (c), 1.5 μs (d), 5.0 μs (e), and 50 μs (f) after photodissociation of CO from cytochrome a_3.

from the mixed-valence complex. In the Soret region (Fig. 1) the trough at 429 nm is due to bleaching of the cytochrome a_3–CO absorbance, and the peak at 446 nm is due to the appearance of unliganded cytochrome a_3^{2+}. Similarly, in Fig. 2, the troughs at ≈588 nm and ≈545 nm observed 10 ns after CO photolysis are due to bleaching of the cytochrome a_3–CO α and β bands, respectively, and the peaks at ≈609 nm and ≈568 nm are due to the α and β bands of the unliganded photoproduct. There is a clear increase in the 370- to 415-nm and the 470- to 550-nm regions with maxima around 390 nm and 520 nm, respectively. Both transients appear as positive absorbances on a microsecond time scale ($t_{1/2} \approx 2$ μs). These changes were not observed after photodissociation of CO from the fully reduced CO-bound enzyme (not shown) and therefore are attributed to intramolecular electron transfer. Fig. 2 shows a blue shift in the cytochrome a_3 α band from 609 to 606 nm and a corresponding shift in the β band. A 2-nm blue shift is observed in the 520-nm band in the 50-μs spectrum. This is clear in the double difference spectrum in Fig. 3, which has a derivative shape for both the α and β band in addition to a broad positive feature at 515 nm. The β band does not show a clear peak but rather a shoulder due to the underlying 520-nm band. The origin of this blue shift is unknown, but it may be due to ligand and/or electron transfer. Accompanying the blue shift, there is a small increase in the α band, which may be due to reduction of cytochrome *a* (*vide infra*). The double difference in the Soret region is not shown, but the broad 390-nm feature is evident in Fig. 1.

The absorbance change at 520 nm in the time-resolved difference spectra in Fig. 2 can be attributed at least partially to the reduction of cytochrome *a*. This is supported by the cytochrome a^{2+}-minus-cytochrome a^{3+} difference spectrum, which shows a small maximum at ≈520 nm (9). However, a reduction of cytochrome *a* corresponding to the absorbance changes observed at 520 nm would be expected to result in a significant increase in the α band, where cytochrome a^{2+} is the major contributor. This is clearly not the case in Fig. 2, where only a very small increase in the α band accompanies the blue shift. This suggests that at least part of the absorbance increase at 520 nm may be due to another chromophore (*vide infra*).

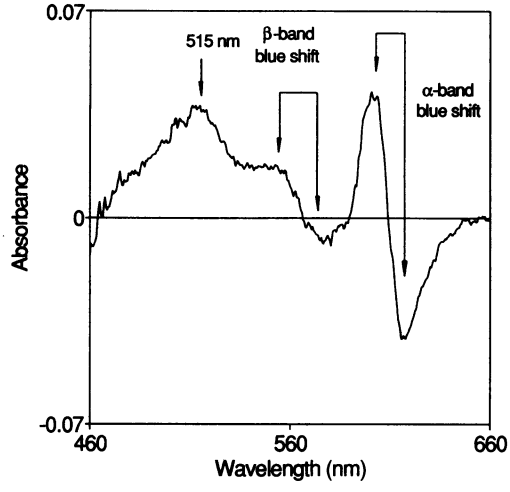

FIG. 3. The transient double difference spectrum of the 50-μs spectrum minus the 10-ns spectrum displayed in Fig. 2.

To determine the contribution of the cytochrome *a* reduction at 520 nm, we have estimated the fraction of cytochrome *a* being reduced on a microsecond time scale from the changes in the α band. The reduction of cytochrome *a* is in fact larger than suggested by the small increase in the α band (Fig. 2) due to compensatory changes occurring at cytochrome a_3^{2+} on the same time scale. We have previously observed that after photodissociation of CO from the fully reduced enzyme, there is ≈30% decrease in the absorbance of the α band (ref. 10; and Ó.E., T.D.D., and K.E.G., unpublished data). These changes, which are on the same time scale ($t_{1/2} \approx 1$ μs) as the loss of CO from Cu_B^+ shown by time-resolved infrared spectroscopy (11), have been ascribed to structural changes at cytochrome a_3 upon dissociation of the Cu_B^+–CO complex (10). It is anticipated that these same structural changes occur at cytochrome a_3 after photolysis of CO from the mixed-valence enzyme. Therefore, to determine the absorbance increase in the α band due to a reduction of cytochrome *a* (Fig. 2), one needs to correct for the absorbance decrease in this region due to structural changes at cytochrome a_3. Including this correction and using the absorbance coefficient (reduced minus oxidized) of 20.5 $mM^{-1}\cdot cm^{-1}$ at 605 nm for cytochrome a^{2+} (9), we calculate that ≈9% of the cytochrome a^{2+} becomes reduced on a microsecond time scale after photodissociation of CO from the mixed-valence complex. These calculations include normalization of our time-resolved difference spectra to 100% photolysis (from ≈60%), since only molecules that undergo photolysis—i.e., have a change in the reduction potential upon CO photodissociation—are expected to undergo a redox-state change. By using an extinction coefficient of the reduced-minus-oxidized cytochrome *a* at 520 nm, $\varepsilon \approx 3000$ $M^{-1}\cdot cm^{-1}$ (9), the 9% reduction of cytochrome *a* corresponds to approximately one-third (36%) of the absorbance increase observed at 520 nm on a microsecond time scale.

The above calculations suggest that ≈64% of the absorbance change at 520 nm corresponds to another chromophore(s). Oxidized cytochrome a_3 does not contribute significantly at this wavelength (9). The position of the 520-nm band (and the 390-nm band), the broad bandwidth, and the extinction coefficient of the change not attributed to cytochrome *a* ($\varepsilon \approx 5400$ $M^{-1}\cdot cm^{-1}$; *vide infra*) is not unusual for charge-transfer transitions involving copper(II), such as those observed for the blue copper proteins plastocyanin, azurin, and stellacyanin (12, 13). It is clear that an extinction coefficient of 5400 $M^{-1}\cdot cm^{-1}$ or greater is too large to be due to copper $d \rightarrow d$ transitions. As mentioned above, the time scale of these absorbance changes is the same as the half-life of the dissociation of CO from Cu_B^+ ($t_{1/2} \approx 1.5$ μs) in the fully reduced cytochrome oxidase as observed by time-resolved infrared spectroscopy (11). After dissociation of CO from Cu_B^+, this metal center would be capable of electron transfer to cytochrome *a* and/or Cu_A. Therefore, we suggest that two-thirds of the absorbance increase at 520 nm may be due to a charge transfer involving Cu_B^{2+}, which appears upon oxidation of Cu_B^+ to Cu_B^{2+}. The extinction coefficient of 5400 $M^{-1}\cdot cm^{-1}$ calculated for this transition is a lower limit, since it assumes a 1:1 electron-transfer stoichiometry between Cu_B and cytochrome *a* (i.e., that cytochrome *a* gets reduced with electrons donated exclusively by Cu_B^+). However, if there were a simultaneous electron transfer from cytochrome a_3 as suggested by a decrease at 446 nm (Fig. 1) and an increase at 670 nm (not shown) on the same time scale, this extinction coefficient would become larger. The copper protein nitrous oxide reductase has been shown to have an intense absorbance ($\varepsilon \approx 16.3$ $mM^{-1}\cdot cm^{-1}$) at 540 nm (14). Recent results obtained in our laboratory suggest that Cu_A is reduced on a later time scale ($t_{1/2} \approx 50$–100 μs) after photolysis of CO from the mixed-valence complex (Ó.E., T.D.D., and K.E.G., unpublished data). These results together with the present data suggest that Cu_A is the primary acceptor of electrons in the forward direction from cytochrome *c*, in agreement with recent work of Oliveberg and Malmström (6) and Hill (15).

The absorbance change at 390 nm exhibits identical kinetic behavior as the 520-nm band and, therefore, may be associated with the same chromophore(s). Also, the 390-nm band is considerably broader than typical heme absorption bands. However, because of a possible contribution of both cytochrome *a* and cytochrome a_3 in the 390-nm region, we are not able to assign a reliable extinction coefficient to the 390-nm band, although it appears to be considerably greater than at 520 nm. We tentatively assign part of this absorbance change to a charge-transfer transition involving Cu_B^{2+}. Fairly intense copper charge-transfer transitions have been reported in the Soret region for copper(II) model compounds (16).

Boelens *et al.* (3) have reported that after photodissociation of CO from the mixed-valence complex, there is a reverse electron flow from cytochrome a_3 to Cu_A ($k_{app} = 7000$ s^{-1}). Brzezinski and Malmström (4) have observed the same process albeit with a higher rate constant ($k_{app} = 14{,}000$ s^{-1}). These authors reported that this process was followed by the reduction of cytochrome *a* at an apparent rate of 500 s^{-1}. Recent studies by Oliveberg and Malmström on the electron transfer in cytochrome oxidase after photolysis of CO from two and three electron-reduced enzyme complexes have suggested that the slow rate, 500 s^{-1}, is due to a structural rearrangement rather than internal electron transfer (6). This study also reports two rapid kinetic phases at both 445 and 605 nm with rate constants of 2×10^5 s^{-1} ($t_{1/2} \approx 3.0$ μs) and 1.3×10^4 s^{-1} ($t_{1/2} \approx 50$ μs), which the authors attribute to internal electron transfer between the bimetallic cytochrome a_3/Cu_B center and cytochrome *a* and between cytochrome *a* and Cu_A, respectively. As evident from Fig. 2, the absorbance increase reported by these authors at 605 nm using single wavelength detection is not an actual increase but is observed because of the blue shift of the α band. The fast phase ($t_{1/2} \approx 3.5$ μs) observed at 445 nm in this study (6) has the same half-life as the transients we observe at 390 and 520 nm. We observe a small decrease in the trough at 429 nm in the time-resolved difference spectra (Fig. 1) on the same time scale as the changes in the α band and the 520- and the 390-nm bands. These changes are most probably due to the reduction of cytochrome a^{3+}, which absorbs at 426 nm (9).

Fig. 2 shows a decrease at 445 nm on a microsecond time scale subsequent to CO photolysis. Since both cytochromes absorb at 445 nm in their reduced forms, determination of the extent of electron transfer between the two hemes in this

region is more difficult. This is further complicated by a small decrease observed at 445 nm after photolysis of CO from the fully reduced enzyme (Ó.E., T.D.D., and K.E.G., unpublished data), which is also expected upon photodissociation of CO from the mixed-valence complex. This transient change is attributed to structural changes at cytochrome a_3 in analogy with the changes observed in the α band on this time scale (*vide supra*).

Preliminary singular value decomposition (SVD) analysis on the Soret difference spectra in Fig. 1 indicates that we have at least four kinetic processes with $t_{1/2}$ values of ≈100 ns, ≈2 μs, ≈85 μs, and ≈12 ms. The origin of the first phase is unknown, but it may represent a submicrosecond process involving cytochrome *a*. This is supported by the 10-ns transient difference spectrum of the CO-photodissociated mixed valence complex (Fig. 2, curve a), which is significantly blue-shifted (≈4 nm) from the 10-ns difference spectrum obtained after photodissociation of CO from the fully reduced enzyme (not shown). The second phase from the SVD analysis has the same lifetime as the processes we observe at 520 and 390 nm. The third phase, which has a half-life of ≈75 μs, may correspond to the 50-μs phase observed by Oliveberg and Malmström (6), which they have attributed to the oxidation of cytochrome *a* upon electron transfer to Cu_A^{2+}. This is in accordance with our observations of an absorbance decrease at 830 nm on this time scale (Ó.E., T.D.D., and K.E.G., unpublished results). The last phase corresponds to the recombination of CO with cytochrome a_3. We observed larger absorbance changes at 830 nm after photodissociation of CO from the three electron-reduced enzyme compared with the mixed-valence enzyme (not shown), in agreement with the studies of Oliveberg and Malmström (6). However, Morgan *et al.* (5) did not find evidence for electron transfer from the binuclear cytochrome a_3/Cu_B site to Cu_A or cytochrome *a* in the mixed-valence CO complex but did report electron transfer (k_{app} = 17,000 s^{-1}, $t_{1/2}$ ≈ 40 μs) between cytochrome *a* and Cu_A in the three electron-reduced enzyme.

The different rates of electron transfer reported by Boelens and Wever (2) and Malmström and coworkers (4, 6) have been suggested to be due to differences in the temporal widths and energy of the excitation pulses used in these experiments (5). Indeed, we have observed (10) that the rate of recombination of CO with cytochrome a_3^{2+} can be accelerated by increasing the probe light intensity of the transient spectrophotometer. We suggested that this was due to photodissociation of a transient cytochrome a_3^{2+}–L complex, where L is a ligand transferred from Cu_B^+ to cytochrome a_3^{2+} upon CO binding to Cu_B^+ (10). The view that a photolabile transient is formed after photodissociation of CO from fully reduced cytochrome *c* oxidase is supported by time-resolved resonance Raman results (10). It is quite possible that these photochemically engendered ligand-exchange reactions may have a significant effect upon electron-transfer rates.

The above results suggest a previously unsuspected intermediate involving Cu_B in the electron-transfer reactions after photodissociation of mixed-valence CO–cytochrome oxidase. Moreover, the similarities of the time scales of the dissociation of CO from Cu_B^+ and the observed electron transfer rates suggest that the rate of electron transfer from Cu_B^+ to cytochrome *a* may be rate-limited by the dissociation of CO from Cu_B^+. This is an important result with respect to electron-transfer studies on partially reduced CO-bound enzyme derivatives and also to previous "flow-flash" experiments that use the photolability of the heme–CO complex to initiate redox reactivity with O_2 (17–21). Further transient UV-visible studies on the electron transfer in cytochrome oxidase on time scales of nanoseconds to milliseconds are expected not only to clarify these issues but also more importantly to elucidate the role of fast ligation, ligand transfer, and electron transfer in the functional dynamics of cytochrome oxidase. Previously, it has invariably been assumed that Cu_B is spectrophotometrically "invisible" because it has only weak $d \rightarrow d$ electronic transitions. Our results suggest that this may not be the case; that relatively strong charge-transfer transitions involving Cu_B^{2+} may exist and may allow direct observation of the behavior of this metal center. In addition, the positions and the intensities of these absorbances may give new insight into the ligand environment of Cu_B.

Acknowledgement is made to the donors of The Petroleum Research Fund, administered by the American Chemical Society, for partial support of this research.

1. Wikström, M., Krab, K. & Saraste, M. (1981) *Cytochrome Oxidase—A Synthesis* (Academic, New York).
2. Boelens, R. & Wever, R. (1979) *Biochim. Biophys. Acta* **547**, 296–310.
3. Boelens, R., Wever, R. & Van Gelder, B. F. (1982) *Biochim. Biophys. Acta* **682**, 264–272.
4. Brzezinski, P. & Malmström, B. G. (1987) *Biochim. Biophys. Acta* **894**, 29–38.
5. Morgan, J. E., Li, P. M., Jang, D.-J., El-Sayed, M. A. & Chan, S. I. (1989) *Biochemistry* **28**, 6975–6983.
6. Oliveberg, M. & Malmström, B. G. (1991) *Biochemistry* **30**, 7053–7057.
7. Yoshikawa, S., Choc, M. G., O'Toole, M. C. & Caughey, W. S. (1977) *J. Biol. Chem.* **252**, 5498–5508.
8. Goldbeck, R. A., Dawes, T. D., Milder, S. J., Lewis, J. W. & Kliger, D. S. (1989) *Chem. Phys. Lett.* **156**, 545–549.
9. Vanneste, W. H. (1966) *Biochemistry* **5**, 838–848.
10. Woodruff, W. H., Einarsdóttir, Ó., Dyer, R. B., Bagley, K. A., Goldbeck, R. A., Dawes, T. D. & Kliger, D. S. (1991) *Proc. Natl. Acad. Sci. USA* **88**, 2588–2592.
11. Dyer, R. B., Einarsdóttir, Ó., Killough, P. M., López-Garriga, J. J. & Woodruff, W. H. (1989) *J. Am. Chem. Soc.* **111**, 7657–7659.
12. Gray, H. B. & Solomon, E. I. (1981) in *Copper Proteins*, ed. Spiro, T. G. (Wiley Interscience, New York), pp. 1–39.
13. Solomon, E., Hare, J. W., Dooley, D. M., Dawson, J. H., Stephens, P. J. & Gray, H. B. (1980) *J. Am. Chem. Soc.* **122**, 168–177.
14. Coyle, C. L., Zumft, W. G., Kroneck, P. M. H., Körner, H. & Jacob, W. (1985) *Eur. J. Biochem.* **153**, 459–467.
15. Hill, B. C. (1991) *J. Biol. Chem.* **266**, 2219–2226.
16. Amundsen, A. R., Whelan, J. & Bosnich, B. (1977) *J. Am. Chem. Soc.* **99**, 6730–6739.
17. Gibson, Q. H. & Greenwood, C. (1963) *Biochem. J.* **86**, 541–554.
18. Chance, B., Saronio, C. & Leigh, J. S., Jr. (1975) *J. Biol. Chem.* **250**, 9226–9237.
19. Clore, G. M., Andréasson, L.-E., Karlsson, B., Aasa, R. & Malmström, B. G. (1980) *Biochem. J.* **185**, 139–154.
20. Babcock, G. T., Jean, J. M., Johnston, L. N., Palmer, G. W. & Woodruff, W. H. (1984) *J. Am. Chem. Soc.* **106**, 8305–8306.
21. Hill, B. C., Greenwood, C. & Nicholls, P. (1986) *Biochim. Biophys. Acta* **853**, 91–113.